Electrochemical properties of $[Fe^{III}(L)_2Cl_2][PF_6]$ and $[Fe_2^{III,III}O(L)_4Cl_2][PF_6]_2$ [L = 2,2′-bipyridine (bpy) and 4,4′-dimethyl-2,2′-bipyridine (dmbpy)]. Crystal structures of the dmbpy derivatives

Marie-Noëlle Collomb,*[a] Alain Deronzier,*[a] Karine Gorgy,[a] Jean-Claude Leprêtre[a] and Jacques Pécaut[b]

[a] *Laboratoire d'Electrochimie Organique et de Photochimie Rédox (CNRS UMR 5630), Université Joseph Fourier, BP 53, 38041 Grenoble cedex 9, France. Fax 33 4 76 51 42 67; E-mail: Alain.Deronzier@ujf-grenoble.fr*

[b] *CEA, Département de Recherche Fondamentale sur la Matière Condensée, Service de Chimie Inorganique et Biologique, Laboratoire de Chimie de Coordination (CNRS URA 1194), CEA/Grenoble, 38054 Grenoble cedex 9, France.*

Received (in Montpellier, France) 9th March 1999, Accepted 12th May 1999

The electrochemical behaviour of the iron(III) complexes $[Fe(L)_2Cl_2]^+$ and $[Fe_2O(L)_4Cl_2]^{2+}$ [L = 2,2′-bipyridine (bpy) and 4,4′-dimethyl-2,2′-bipyridine (dmbpy)] has been investigated in acetonitrile. Their reduction leads to the iron(II) complex ion $[Fe(L)_3]^{2+}$, accompanied by the release of Cl^- ions and the formation of $[FeCl_4]^-$ ions or by the formation of an unidentified Fe(III) chloro oxide, depending on the starting complex. These two new chloro complexes can be further reduced into Fe(II) species at a more negative potential. In addition, it has been shown that $[Fe(L)_2Cl_2]^+$ can be obtained in good yield *via* the electrochemical oxidation of $[Fe(L)_3]^{2+}$ in the presence of free Cl^- anions, at least for L = dmbpy. The crystal structure of the new mono- and binuclear dmbpy complexes has been determined by X-ray diffraction.

Products formed by reaction of iron(III) chloride with bidentate nitrogen ligands (L) like 1,10-phenanthroline (phen) and 2,2′-bipyridine (bpy) have been widely studied in the past six decades[1–11] using several synthetic and physical procedures. However, only a few of the resulting compounds, such as $[Fe(L)_2Cl_2][FeCl_4]$,[12–14] $[FeCl_3(phen)X]$[15] (X = MeOH, H_2O, Cl^-), $[Fe(bpy)_3][Cl_3FeOFeCl_3]$[16] and $[Fe_2O(phen)_4Cl_2][Cl_2]$,[16] have been fully characterized, in particular with the help of crystallographic studies. On the other hand, until now the electrochemical properties of this kind of complex have remained unknown. We have recently reported a detailed study on the electrochemical behaviour of the parent binuclear bisaqua complexes $[Fe_2O(L)_4(H_2O)_2]^{4+}$ in organic solvent[17] (CH_3CN). These bisaqua complexes constitute excellent structural models of diiron sites in proteins involved in the reductive activation of molecular oxygen. Furthermore, they act as efficient catalysts for the oxidation of alkanes in the presence of oxygen atom donors whereas the bischloro analogues are poor catalysts.[18]

In this context we have studied the electrochemical behaviour of the mononuclear $[Fe^{III}(L)_2Cl_2]^+$ and the binuclear monobridged $[Fe_2^{III,III}O(L)_4Cl_2]^{2+}$ complexes [L = 2,2′-bipyridine (bpy) and 4,4′-dimethyl-2,2′-bipyridine (dmbpy)]. These complexes have been synthesized as PF_6^- or BF_4^- salts since $FeCl_4^-$ and Cl^- are electroactive anions. To help in the understanding of the electrochemical mechanisms, the redox properties of $FeCl_3$ and $FeCl_4^-$ have been revisited first. Moreover, the crystal structures of the new dmbpy derivatives $[Fe^{III}(dmbpy)_2Cl_2][PF_6]$ and $[Fe_2^{III,III}O(dmbpy)_4Cl_2][PF_6]_2$ have also been determined by single-crystal X-ray diffraction experiments at 295 K.

Experimental

Elemental analyses were performed by the Service Central d'Analyse du CNRS at Vernaison (France).

Materials

Anhydrous $FeCl_3$, stocked under inert atmosphere (Acros, 98%), 2,2′-bipyridine (bpy, Aldrich, 99%), 4,4′-dimethyl-2,2′-bipyridine (dmbpy, Fluka, 99%), tetraethylammonium chloride (Et_4NCl, Fluka, 99%), tetrabutylammonium chloride (Bu_4NCl, Fluka, 99%), tetrabutylammonium tetrafluoroborate (NBu_4BF_4, Fluka, 99%) and tetrabutylammonium hexafluorophosphate (NBu_4PF_6, Fluka, 99%) were used as received.

Synthesis and characterization

$[Fe(L)_2Cl_2][PF_6]$ (L = bpy and dmbpy). To a 10 ml solution of 270 mg of $FeCl_3$ (1 mmol), 312 mg of bpy or 368 mg of dmbpy were added. The resulting solution, which turned dark orange upon addition of the ligand, was stirred for 15 min. Then, 1.93 g of Bu_4NPF_6 was added to the resulting solution, leading to the precipitation of a yellow product. The solid was collected on a frit, washed successively with methanol (3 × 30 ml) and diethyl ether (3 × 30 ml) and dried *in vacuo*. In order to prevent the cocrystallisation of $[Fe(L)_2Cl_2]^+$ with $FeCl_4^-$ as the counter anion, the yellow solids were recrystallized from MeOH–CH_3CN (2 : 1). Yellow crystals of $[Fe(bpy)_2Cl_2][PF_6]$ (294 mg, yield 50.4%) and $[Fe(dmbpy)_2Cl_2][PF_6]$ (405 mg, yield 69%) were obtained after one or two days. Only

crystals of the dmbpy derivatives have been crystallographically characterized. Anal. calcd for $C_{20}H_{16}N_4Cl_2F_6FeP$: C, 45.64; H, 3.04; N, 10.65; Fe, 10.62. Found: C, 45.69; H, 3.27; N, 10.65; Fe, 9.84%. UV/Vis (CH_3CN) λ_{max}/nm (ε/M^{-1} cm^{-1}): 362 (5200). Anal. calcd for $C_{24}H_{24}N_4Cl_2F_6FeP$: C, 45.01; H, 3.75; N, 8.75; Fe, 8.72. Found: C, 44.75; H, 3.91; N, 8.86; Fe, 8.16%. UV/Vis (CH_3CN) λ_{max} nm (ε/M^{-1} cm^{-1}) 362 (5500).

$[Fe_2O(L)_4Cl_2][PF_6]_2$ (L = bpy and dmbpy). These complexes were prepared following a method similar to that of literature.[18] To a 10 ml solution of 516 mg of $Fe(ClO)_4 \cdot 9H_2O$ (1 mmol), 1 equiv. of Bu_4NCl (277.5 mg) was added. Then 2 equiv. of bpy (312 mg) were added, leading to the formation of a brown precipitate. After addition of 1.93 g of Bu_4NPF_6 (5 mmol), the reaction mixture was refluxed for 1 h in order to dissolve the precipitate. The solution was then cooled to room temperature and the pale brown product obtained was filtered off, dried *in vacuo* and recrystallized from MeOH–CH_3CN (9 : 1). Yield 300 mg (53%).

For L = dmbpy, the same procedure was followed except that 1 equiv. of triethylamine (140 ml) was added after the addition of 368 mg of dmbpy. Small pale brown crystals of $[Fe_2O(dmbpy)_4Cl_2][PF_6]_2$ suitable for X-ray diffraction analysis were obtained by two successive recrystallizations from MeOH–CH_3CN (1 : 1). Yield 257 mg (42%).

The synthesis of such complexes with BF_4^- as counter anions has been performed by using Bu_4NBF_4 instead of Bu_4NPF_6.

Crystal structure resolution and refinement

The data sets for the single-crystal X-ray studies were collected with MoKα radiation on a Brucker SMART diffractometer. All calculations were performed on a Silicone graphic system, using the SHELXTL program.[19] The specific data for the crystals and the refinements are collected in Table 1. The structures were solved by direct methods and refined by full-matrix least-squares on F_2.

CCDC reference number 440/120. See http://www.rsc.org/suppdata/nj/1999/785/ for crystallographic files in .cif format.

Electrochemical and spectroscopic studies

All electrochemical experiments were run under an argon atmosphere in a glove-box at room temperature. Acetonitrile (CH_3CN, Rathburn, HPLC grade) was used as received and stocked under an argon atmosphere in the glove box. The supporting electrolyte, tetra-*n*-butylammonium perchlorate (TBAP) was purchased from Fluka, recrystallized from ethyl acetate–cyclohexane and dried under vacuum at 80 °C for 3 days.

Cyclic voltammetry and controlled potential electrolysis experiments were performed using a PAR model 273 potentiostat/galvanostat or a PAR model 173 potentiostat/galvanostat, a PAR model 175 universal programmer and a PAR model 179 digital coulometer. The standard three-electrode electrochemical cell was used. Potentials are reference to an Ag|10 mM $AgNO_3$ reference electrode in CH_3CN + 0.1 M TBAP. Potentials referenced to that system can be converted to the ferrocene|ferrocenium couple by adding 70 mV. The working electrodes were a platinum and vitreous carbon disc (5 mm diameter) polished with 1 μm diamond paste. Exhaustive electrolyses were carried out with a $10 \times 10 \times 4$ mm^3 carbon felt electrode (RCV 2000, 65 mg cm^{-3}, from Le Carbone Lorraine).

Electronic absorption spectra were recorded on a Hewlett–Packard 8452A diode array spectrophotometer controlled by a Compacq 286 computer. Initial and electrolyzed solutions were transferred to a conventional cuvette cell in the glove box. The cell was inserted into an optical translator connected to the spectrophotometer through a fibre optic system (Photonetics Spectrofip System). The optical fibres pass through the wall of the dry box *via* optical seals.

Results and discussion

Description of the crystal structures

$[Fe^{III}(dmbpy)_2Cl_2][PF_6]$. The molecular structure of $[Fe(dmbpy)_2Cl_2]^+$ is presented in Fig. 1, while relevant bond lengths and angles are compiled in Table 2. The coordination of four N atoms from the two dmbpy ligands and two Cl ions to the central Fe atom produces a distorted octahedron with the two Cl atoms in a *cis* arrangement. The average of the Fe–Cl bond lengths [2.2651(6) Å] compares well with those reported for the two polymorphs of $[Fe(bpy)_2Cl_2][FeCl_4]$ (2.255 Å[14] and 2.258 Å[12,13]), as well as for the phen complex

Table 1 Crystal data and details of the refinement of the crystal structures of $[Fe(dmbpy)_2Cl_2][PF_6]$ and $[Fe_2O(dmbpy)_4Cl_2][PF_6]_2$. Standard deviations are given in parentheses

	$[Fe(dmbpy)_2Cl_2][PF_6]$	$[Fe_2O(dmbpy)_4Cl_2][PF_6]_2$
Chemical formula	$C_{24}H_{24}Cl_2F_6FeN_4P$	$C_{48}H_{48}Cl_2F_{12}Fe_2N_8OP_2$
Formula weight	640.19	1225.48
T/K	193(2)	193(2)
Crystal system	Orthorhombic	Monoclinic
Space group	*Pbca*	*C*2/*c*
	a/Å 17.0596(2)	*a*/Å 12.5133(8)
	b/Å 11.1202(2)	*b*/Å 27.125(2)
	c/Å 28.8769(4)	*c*/Å 16.0006(10)
	α/° 90	α/° 90
	β/° 90	β/° 92.5290(10)
	γ/° 90	γ/° 90
U/Å^3	5478.13(14)	5425.6(6)
Z	8	4
μ/mm^{-1}	0.867	0.777
No. of reflections collected	23818	12092
No. of independent reflections	4969 (R_{int} = 0.0626)	4717 (R_{int} = 0.1171)
Goodness-of-fit on F^2	1.169	1.012
Final R indices [$I > 2\sigma(I)$]	R_1 = 0.0687	R_1 = 0.0942
	wR_2 = 0.1923	wR_2 = 0.2014
R indices (all data)	R_1 = 0.0883	R_1 = 0.2140
	wR_2 = 0.2060	wR_2 = 0.2586
Largest diff. peak, hole/e Å^{-3}	1.845, −0.669	0.819, −0.835

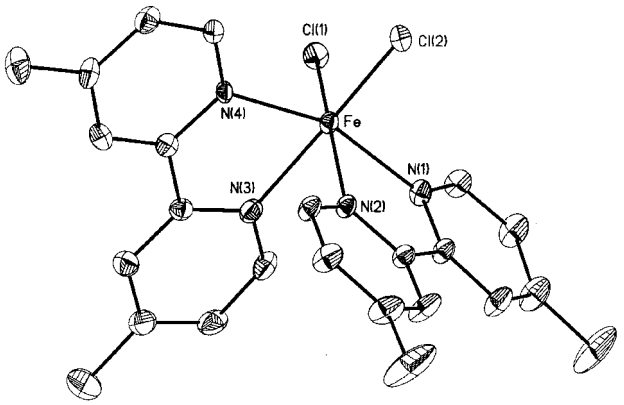

Fig. 1 Molecular structure and atom labelling scheme of $[Fe^{III}(dmbpy)_2Cl_2]^+$.

$[Fe(phen)_2Cl_2][FeCl_4]$ (2.258 Å[13]). The Fe–N bond distances *trans* to Cl [average 2.204(2) Å] are significantly longer than the Fe–N bond distances *cis* to Cl [average 2.1305(2) Å]. This result is also consistent with the Fe–N bond distances found in the analogous bpy complexes (2.193, 2.121 Å[14] and 2.176, 2.136 Å[12,13]) and the phen one (2.206, 2.136 Å[13]).

$[Fe_2^{III,III}O(dmbpy)_2Cl_2][PF_6]_2$. The molecular structure of $[Fe_2O(dmbpy)_4Cl_2]^{2+}$ is shown in Fig. 2, selected bond lengths and angles are listed in Table 3. The Fe atoms are each coordinated by four N atoms provided by two dmbpy ligands and by the bridging O atom of the bridge. The sixth coordination site is occupied by a Cl ligand *cis* to the oxo

Table 2 Selected bond lengths (in Å) and bond angles (in degrees) for $[Fe(dmbpy)_2Cl_2][PF_6]$

2-atom data			
Fe–Cl(1)	2.2630(6)	Fe–N(2)	2.213(2)
Fe–Cl(2)	2.2673(6)	Fe–N(3)	2.195(2)
Fe–N(1)	2.133(2)	Fe–N(4)	2.128(2)
3-atom data			
Cl(1)–Fe–Cl(2)	99.69(2)	Cl(2)–Fe–Cl(4)	96.55(4)
Cl(1)–Fe–N(1)	96.45(5)	N(1)–Fe–N(2)	75.18(6)
Cl(1)–Fe–N(2)	169.17(5)	N(1)–Fe–N(3)	88.60(7)
Cl(1)–Fe–N(3)	90.93(5)	N(1)–Fe–N(4)	159.33(6)
Cl(1)–Fe–N(4)	97.55(5)	N(2)–Fe–N(3)	82.14(6)
Cl(2)–Fe–N(1)	96.01(5)	N(2)–Fe–N(4)	88.87(6)
Cl(2)–Fe–N(2)	88.16(5)	N(3)–Fe–N(4)	76.05(6)
Cl(2)–Fe–N(3)	167.85(5)		

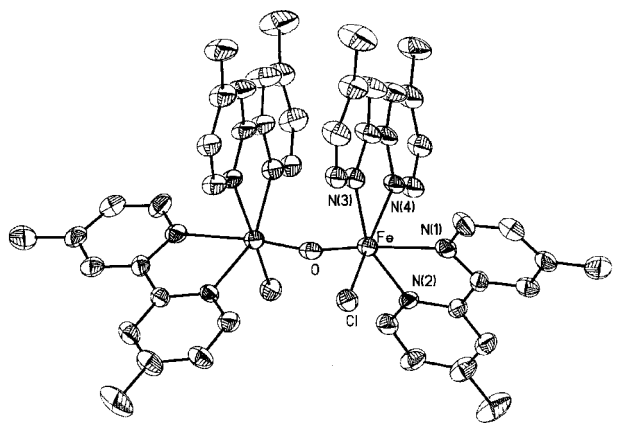

Fig. 2 Molecular structure and atom labelling scheme of $[Fe_2^{III,III}O(dmbpy)_4Cl_2]^{2+}$.

Table 3 Selected bond lengths (in Å) and bond angles (in degrees) for $[Fe_2O(dmbpy)_4Cl_2][PF_6]_2$

2-atom data			
Fe–N(1)	2.216(8)	Fe–Cl	2.328(3)
Fe–N(2)	2.155(6)	Fe–O	1.786(2)
Fe–N(3)	2.154(6)	O–Fe #1	1.786(2)
Fe–N(4)	2.191(6)		
3-atom data			
Fe–O–Fe #1	167.4(4)	O–Fe–N(1)	167.7(2)
Cl–Fe–O	100.27(14)	N(4)–Fe–N(1)	85.5(2)
Cl–Fe–N(4)	165.2(2)	N(3)–Fe–N(1)	89.0(3)
O–Fe–N(4)	90.6(2)	Cl–Fe–N(2)	99.7(2)
Cl–Fe–N(3)	93.1(2)	O–Fe–N(2)	94.7(3)
O–Fe–N(3)	101.2(3)	N(4)–Fe–N(2)	89.4(2)
N(4)–Fe–N(3)	74.8(2)	N(3)–Fe–N(2)	157.5(3)
Cl–Fe–N(1)	85.9(2)	N(1)–Fe–N(2)	73.6(3)

bridge. Bond angles suggest that the octahedron at each Fe centre is distorted (Table 3). The Fe–O–Fe angle [167.4(4)°] is close to those observed for the bishydroxy mono-oxo-bridged complex of Fe^{III} (161.7°)[20] and for $[Fe_2O(phen)_4Cl_2]^{2+}$ [161(1)°][16]. Moreover, the bond lengths found in this cation do not differ significantly from those of $[Fe_2O(phen)_4Cl_2]^{2+}$.[16]

The Fe–O distance of 1.786(2) Å for the oxo bridge is consistent with the value of 1.787(6) Å observed in the phen complex[16] and is also comparable to those found in other similar mono-oxo-bridged complexes of Fe^{III}.[20] The Fe–Cl bond length [2.328(3) Å] compares well with that observed in the phen complex[16] [2.34(1) Å] but is longer than the ones in the monomeric $[Fe(L)_2Cl_2]^+$ cations (L = bpy, dmbpy, phen). Moreover, for the Fe–N distances, the two longer bonds are found for the two N atoms *trans* to the oxo bridge [2.216(8) Å], reflecting the *trans* effect. A slightly smaller effect is observed for the Fe–N bonds *trans* to the Cl ligands [2.191(6) Å].

Electrochemistry

Electrochemical behaviour of $FeCl_3$ and $FeCl_4^-$. In CH_3CN + 0.1 M TBAP, the cyclic voltammogram (CV) of a 1.2 mM solution of anhydrous $FeCl_3$ shows in the negative region two successive quasi-reversible waves located at $E_{1/2} = -0.18$ V ($\Delta E_p = 110$ mV) and $E_{1/2} = -0.32$ V, ($\Delta E_p = 90$ mV) (close to the thermodynamic value of 60 mV for a monoelectronic transfert) at $v = 100$ mV s^{-1} *vs.* Ag|10 mM Ag^+ [Fig. 3(*A*)]. These waves have been briefly reported in a previous work by Sugimoto and Sawyer[21] and attributed to the $Fe^{III}Cl_3/Fe^{II}Cl_3^-$ and $Fe^{III}Cl_4^-/(Fe^{II}Cl_3^- + Cl^-)$ systems, respectively. We will see that $Fe^{II}Cl_4^{2-}$ is a stable species in CH_3CN so the second couple actually corresponds to the $Fe^{III}Cl_4^-/Fe^{II}Cl_4^{2-}$ system.

The addition of increasing amounts of Cl^- anions to the solution results in an increase of the $Fe^{III}Cl_4^-/Fe^{II}Cl_4^{2-}$ wave up to about one molar equivalent [Fig. 3(*B*) and 3(*C*), curve *a*]. If more than one equivalent of Cl^- is added, then the CV displays the typical electroactivity of free Cl^- ions in the positive region[22] (a quasi-reversible system at $E_{p_a} = 0.74$ V; not shown on Fig. 3). All these observations confirm the formation of a 1 : 1 complex between $FeCl_3$ and Cl^-.

The stability of the $Fe^{II}Cl_4^{2-}$ species has been evaluated by an exhaustive reduction at −0.40 V of the solution containing one equivalent of Cl^- : 0.8 electron per molecule of $FeCl_3$ initially present has been consumed as determined by measurement of the height of its wave at a Pt rotating disc electrode and yields about 80% of $FeCl_4^{2-}$ [Fig. 3(*C*), curve *b*].

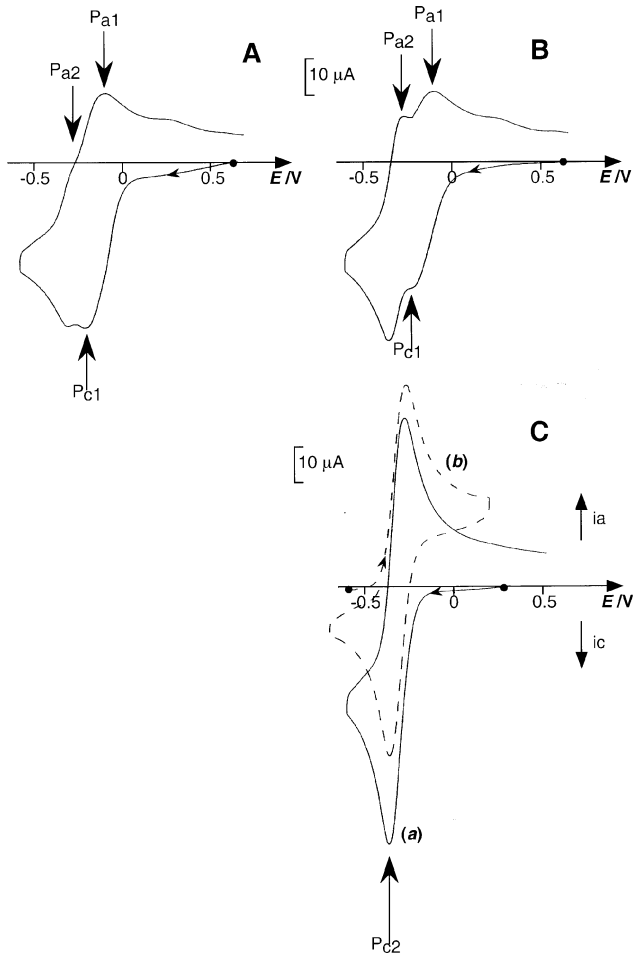

Fig. 3 CV in CH_3CN + 0.1 M TBAP of a 1.2 mM solution of $FeCl_3$ at a platinum electrode (5 mm diameter); scan rate: 100 mV s^{-1}. (*A*) In the absence of Et_4NCl. (*B*) After addition of 0.48 equiv. of Et_4NCl. (*C*) After addition of 1 equiv. of Et_4NCl (curve *a*); after an exhaustive reduction at a controlled potential of −0.4 V of the solution obtained in curve *a* (curve *b*).

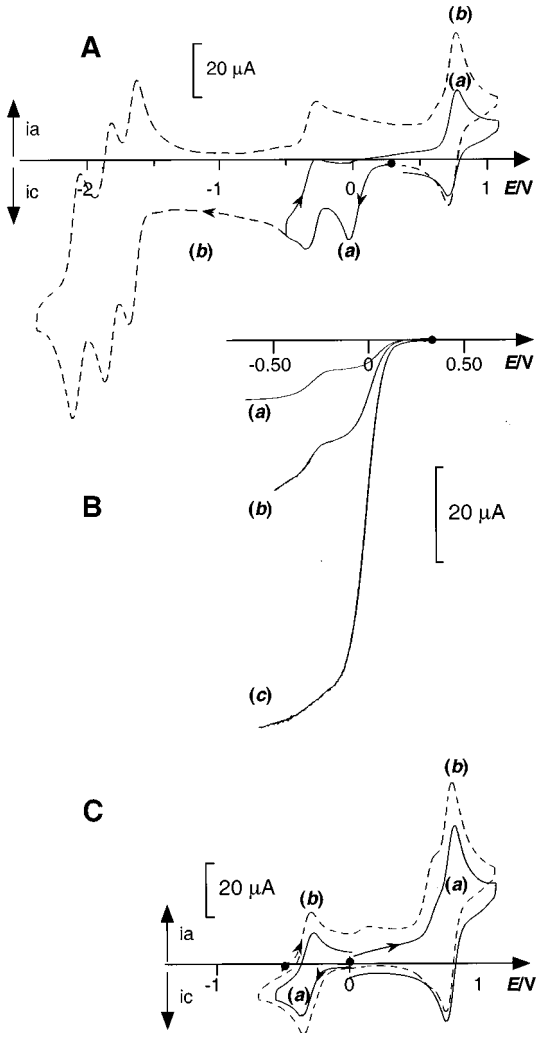

Fig. 4 (*A*) CV in CH_3CN + 0.1 M TBAP at a platinum electrode (5 mm diameter) of a 1 mM solution of $[Fe^{III}(bpy)_2Cl_2]^+$; scan rate: 100 mV s^{-1}; potential range between −0.5 and 1.1 V (curve *a*); potential range between −2.3 and 1.1 V (curve *b*). (*B*) Voltammograms of a 1 mM solution of $[Fe^{III}(bpy)_2Cl_2]^+$ at a platinum rotating disc electrode (2 mm diameter); scan rate: 10 mV s^{-1}; ω = 100 rot min^{-1} (curve *a*), ω = 600 rot, min^{-1} (curve *b*), ω = 5000 rot min^{-1} (curve *c*). (*C*) CV in CH_3CN + 0.1 M TBAP of a 1 mM solution of $[Fe^{III}(bpy)_2Cl_2]^+$ at a platinum electrode (5 mm diameter); scan rate: 100 mV s^{-1}; after an exhaustive reduction at a controlled potential of −0.14 V (curve *a*); after an exhaustive reduction at controlled potential at a −0.4 V of the solution obtained in curve *a* (curve *b*).

Electrochemical properties of $[Fe^{III}(L)_2Cl_2]^+$. Fig. 4(*A*), curve *a* shows the CV of a 1 mM solution of $[Fe^{III}(bpy)_2Cl_2][BF_4]$ in CH_3CN at 100 mV s^{-1}. This complex is not electroactive in the positive region while, in the negative one, an irreversible reduction peak is detected at $E_{p_c} = -0.02$ V followed by a peak system at $E_{1/2} = -0.32$ V, corresponding to the reversible reduction of $Fe^{III}Cl_4^-$ into $Fe^{II}Cl_4^{2-}$. The $Fe^{III}Cl_4^-$ species is generated from a fast chemical reaction coupled to the initial electron transfer. The relative intensity of these two cathodic systems depends on the potential scan rate. This is clearly evidenced by rotating disc electrode experiments. At a low rotation rate [ω = 100 rot min^{-1}, Fig. 4(*B*), curve *a*], the two cathodic waves have roughly the same intensity. At a moderate rotation rate [ω = 600 rot min^{-1}, Fig. 4(*B*), curve *b*], the height of the reduction wave of $FeCl_4^-$ is markedly smaller than that of $[Fe^{III}(bpy)_2Cl_2]^+$ while at 5000 rot min^{-1}, only the $[Fe^{III}(bpy)_2Cl_2]^+$ wave is detected [Fig. 4(*B*), curve *c*]. Otherwise, by sweeping down to −2.3 V [Fig. 4(*A*), curve *b*], the typical three successive ligand-centered reduction waves of $[Fe^{II}(bpy)_3]^{2+}$ are observed on the CV at $E_{1/2} = -1.65$, −1.83 and −2.07 V. This means that $[Fe^{II}(bpy)_3]^{2+}$ is the product of the reduction of $[Fe^{III}(bpy)_2Cl_2][BF_4]$.

On the reverse scan, the reversible oxidation wave of this $[Fe(bpy)_3]^{2+}$ complex is also detected at $E_{1/2} = 0.76$ V in the positive region. This system is accompanied by the quasi-reversible wave at $E_{1/2} = 0.62$ V of Cl^- released during the reduction process. A controlled-potential reduction of the solution at −0.14 V consumes 0.64 electrons per molecule of initial complex. The resulting deep red solution contains 0.64 mM of $[Fe(bpy)_3]^{2+}$ (the amount is evaluated by its typical visible absorption band at 521 nm using an ε value of 8540 M^{-1} cm^{-1}). Besides the reversible peak system of the electrogenerated $[Fe(bpy)_3]^{2+}$ at $E_{1/2} = 0.76$ V, a quasi-reversible one at $E_{1/2} = 0.62$ V is also seen in the positive region, confirming the release of Cl^- ions.

In the negative region, the reversible reduction peak system of $FeCl_4^-$ is present at $E_{1/2} = -0.32$ V. The amount of Cl^- and $FeCl_4^-$ formed after electrolysis can be estimated by the height of their respective waves at a rotating Pt electrode by comparison with data obtained with a pure sample solution of these products. Values are close to 0.55 mM for Cl^- and 0.3 mM for $FeCl_4^-$. Eqn. (1) summarizes the proposed reduction process of $[Fe^{III}(bpy)_2Cl_2]^{2+}$. The experimental values found for the amounts of compound formed are in good agreement with the stoichiometry of the reaction:

$$[Fe^{III}(bpy)_2Cl_2]^+ + \tfrac{2}{3}e^- \rightarrow \tfrac{2}{3}[Fe^{II}(bpy)_3]^{2+} + \tfrac{2}{3}Cl^- + \tfrac{1}{3}[Fe^{III}Cl_4]^- \quad (1)$$

An additional exhaustive reduction carried out at −0.4 V consumes 0.28 electron per molecule of initial $[Fe^{III}(bpy)_2Cl_2]^+$ and reduces $[Fe^{III}Cl_4]^-$ into $[Fe^{II}Cl_4]^{2-}$ as judged by the recorded CV at the end of the electrolysis [Fig. 4(*C*), curve *b*]. Eqn. (2) summarizes the overall process involved in the two successive reductions:

$$[Fe^{III}(bpy)_2Cl_2]^+ + e^- \rightarrow \tfrac{2}{3}[Fe^{II}(bpy)_3]^2 + \tfrac{1}{3}[Fe^{II}Cl_4]^{2-} + \tfrac{2}{3}Cl^- \quad (2)$$

A similar electrochemical behaviour is observed for the parent complex $[Fe(dmbpy)_2Cl_2]^+$. The irreversible reduction of $[Fe(dmbpy)_2Cl_2]^+$ occurs at a more negative potential (E_{pa} = −0.12 V) while the oxidation of the corresponding trischelate complex $[Fe(dmbpy)_3]^{2+}$ occurs at a less positive potential ($E_{1/2}$ = 0.60 V), in accordance with the donor effect produced by the methyl group on the bipyridine ligand.

Finally, we have tried to electrochemically prepare the bischloro complex from the trisbipyridine derivative by its oxidation in the presence of Cl^-. $[Fe(dmbpy)_3]^{2+}$ is a more convenient candidate than $[Fe(bpy)_3]^{2+}$ for this experiment since its oxidation potential is not as close to that of Cl^-. An exhaustive oxidation of a mixed solution of $[Fe(dmbpy)_3]^{2+}$ (10^{-3} M) and Et_4NCl (2.2×10^{-3} M) was carried out at 0.6 V and the applied potential was gradually increased up to 0.8 V. After approximately 1.2 electrons per mole of $[Fe(dmbpy)_3]^{2+}$ had been consumed, all Cl^- were consumed and no $[Fe(dmbpy)_3]^{2+}$ remained, as shown by analysis of the resulting solution by CV and visible spectroscopy. $[Fe(dmbpy)_2Cl_2]^+$ was thus produced in high yield (≈95%). This experiment shows that electrochemistry can be an excellent method to prepare the bischloro derivative and that the Fe^{3+} cation is preferentially coordinated by chloro ligands *vs.* bipyridine ones, in contrast to Fe^{2+}. Eqn. (3) summarizes the electrochemically induced reaction:

$$[Fe^{II}(dmbpy)_3]^{2+} + 2\ Cl^- \rightarrow [Fe^{III}(dmbpy)_2Cl_2]^+ + dmbpy + e^- \quad (3)$$

Electrochemical behaviour of $[Fe_2^{III,III}O(L)_4Cl_2]^{2+}$. As observed previously for the parent binuclear bisaqua complex $[Fe_2O(L)_4(H_2O)_2]^{4+}$,[18] these complexes are not electroactive in the positive region, while in the negative region an irreversible peak is observed (E_{pc} = −0.52 and −0.60 V for L = bpy and dmbpy, respectively). On the reverse scan of the CV [Fig. 5(*A*), curve *a*] the typical reversible wave system of the metal-centred oxidation $Fe^{II/III}$ of the tris-L chelate $[Fe(L)_3]^{2+}$ system appears. Moreover, if the potential is scanned down to −2.3 V, the regular three successive ligand-based reversible reductions of this complex are observed. The reduction of the binuclear complex induces the loss of Cl^- ions as evidenced by the presence of a shoulder on the oxidation peak of $[Fe(bpy)_3]^{2+}$ on the reverse scan [Fig. 5(*A*), curve *b*]. A controlled-potential reduction at (−0.7 V using a carbon felt electrode) of a 1 mM solution of these binuclear complexes yields a deep red solution having the analytical characteristics of a 1.25 mM solution of $[Fe(L)_3]^{2+}$. Besides the reversible system of $[Fe(L)_3]^{2+/3+}$, the quasi-reversible system of Cl^- is also seen on the CV. The amount of Cl^- ions released, as estimated by the height of this wave, is close to 1.3 mM. We suggest that the overall process implied by the reduction of $[Fe_2O(L)_2Cl_2]^{2+}$ is the following:

$$[Fe_2O(L)_4Cl_2]^{2+} + \tfrac{4}{3}e^- \rightarrow \tfrac{4}{3}[Fe(L)_3]^{2+} + \tfrac{4}{3}Cl^- + \ll Fe^{III}\ cloro\ oxide \gg \quad (4)$$

Some amount of iron remains in solution, probably as an unidentified chloro oxide compound of Fe^{III} (the formulation $[Fe_2O_3Cl_2]^{2-}$ can be proposed for the unidentified chloro oxide in order to respect the mass balance). The n_{app} (Faraday per mol of reactant consumed) of 1.21 obtained is in good agreement with the stoechiometry of eqn. (4). No $[FeCl_4]^{2-}$ is detected at the end of the electrolysis, indicating that $[Fe(L)_2Cl_2]^+$ is not formed during the reduction process. A further electrolysis at −1.25 V using the same working electrode allows the consumption of an additional change of 0.82 electron per mol. The total amount of released Cl^- then reaches 2 mM, showing that the chloro oxide iron(III) is reduced. It is interesting to note that the reoxidation at +1 V of the solution does not quantitatively restore the initial binuclear complex and instead gives a mixture of bis- and tris-bpy Fe^{III} complexes. The coulometric excess (n = 2, 4) is probably due to the fact that at this potential, the chloride ions are also oxidized.

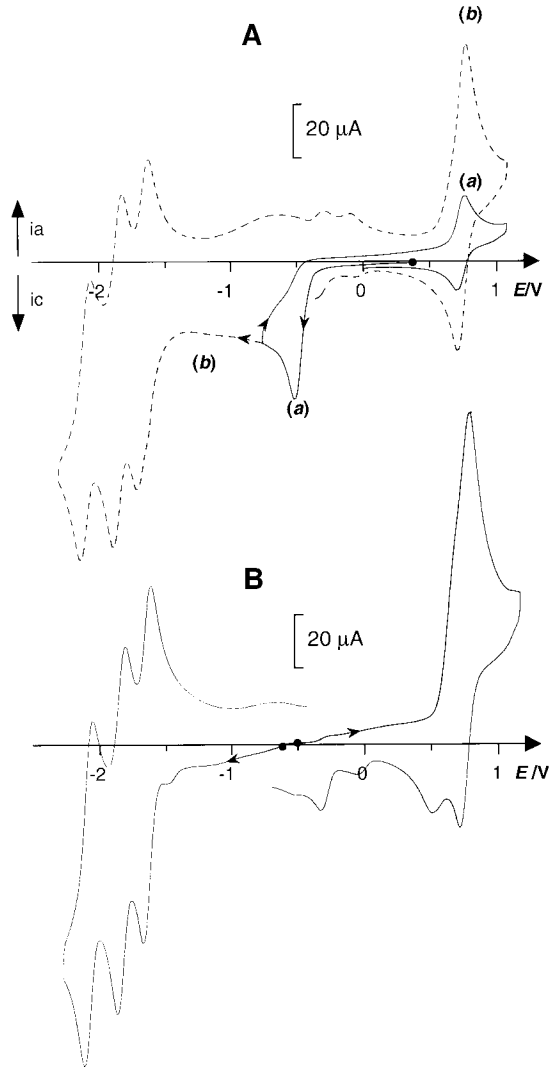

Fig. 5 (*A*) CV in CH_3CN + 0.1 M TBAP of a 1 mM solution of $[Fe_2^{III,III}O(bpy)_4Cl_2]^{2+}$ at a platinum electrode (5 mm diameter); scan rate: 100 mV s^{-1}; potential range between −0.5 and 1.1 V curve (*a*); potential range between −2.3 and 1.1 V curve (*b*). (*B*) After an exhaustive reduction at a controlled potential of −0.7 V.

Correlation with catalytic oxidation

As previously reported the μ oxo bisaqua complex $[Fe_2O(L)_4(H_2O)_2]^{4+}$ represents one of the most efficient non-heme iron catalysts for alkane oxidation by *tert*-butyl hydroperoxide (TBHP) in acetonitrile, whereas the μ-oxo bischloro analogues are significantly less active.[18] The mechanism of the oxidation of cyclohexane, for example, by TBHP with such catalysts is now well documented.[23,24] It appears that the first species formed during the process is an iron–alkyl peroxo complex.[25] The latter is decomposed into alkoxy radicals by homolytic cleavage of the O–O bond able to abstract hydrogen from alkane. Obviously one reason for the difference of activity between the two types of μ-oxo complexes comes from

the lower propensity of the chloro ligands *vs.* aqua ligands to exchange to form an iron–alkyl peroxo complex. On the other hand, an alternative route to form radicals is to consider a heterolytic cleavage of the Fe–OOR bond, leading to the formation of a mononuclear species like $[Fe(L)_2(H_2O)_2]^{2+}$ and peroxyl radicals. We have recently demonstrated that $[Fe(L)_2(H_2O)_2]^{2+}$ is easily quantitatively reoxidized into the initial $[Fe_2O(L)_4(H_2O)_2]^{4+}$ catalyst by TBHP.[17] This present study shows, in contrast, that the reoxidation of the species issued from the reduction of $[Fe_2O(L)_4Cl_2]^{2+}$ does not restore this latter species. This behaviour constitutes another important limitation to the catalytic efficiency of $[Fe_2O(L)_4Cl_2]^{2+}$.

Conclusion

This study shows that the iron(III) complexes $[Fe(L)_2Cl_2]^+$ and $[Fe_2O(L)_4Cl_2]^{2+}$ are electrochemically reduced to $[Fe(L)_3]^{2+}$. Formation of this complex is accompanied by the release of Cl^- ions and the formation of $[FeCl_4]^-$ ions in the case of $[Fe(L)_2Cl_2]^+$ reduction, while an unidentified Fe^{III} chloro oxide species results from the $[Fe_2O(L)_4Cl_2]^{2+}$ reduction. It has also been shown that $[Fe(L)_2Cl_2]^+$ can in turn be electrogenerated by oxidation of $[Fe(L)_3]^{2+}$ in the presence of Cl^- anions. This result indicates that the Fe^{3+} cation is preferentially coordinated by chloro ligands *vs.* bipyridine ones, unlike the Fe^{2+} cation.

Acknowledgements

We thank the Région Rhône-Alpes (Programme Emergence) for partial financial support and Dr. Stéphane Ménage for fruitful discussions.

References

1 A. Gaines, L. P. Hammett and G. H. Walden, *J. Am. Chem. Soc.*, 1936, **58**, 1668.
2 A. Simon, G. Morgenstern and W. H. Z. Albrecht, *Anorg. Allg. Chem.*, 1937, **230**, 225.
3 L. Michaelis and S. Granick, *J. Am. Chem. Soc.*, 1943, **65**, 481.
4 H. Irving, E. J. Buttler and M. F. King, *J. Chem. Soc.*, 1949, 1489.
5 C. M. Harris and T. N. Lockyer, *Chem. Ind.* (*London*), 1958, 1231.
6 A. Earnshaw and J. Lewis, *J. Chem. Soc.*, 1961, 396.
7 G. Anderegg, *Helv. Chim. Acta*, 1962, **45**, 1643.
8 B. N. Figgis and J. Lewis, *Prog. Inorg. Chem.*, 1964, **6**, 168.
9 A. V. Khedekar, J. Lewis, F. E. Mabbs and H. Weigold, *J. Chem. Soc. A*, 1967, 1561.
10 R. R. Berrett, B. W. Fitzsimmons and A. A. Owusu, *J. Chem. Soc. A*, 1968, 1575.
11 S. N. Ghosh, *Indian J. Chem.*, 1975, **13**, 66.
12 H. J. Goodwin, M. Mc Partlin and H. A. Goodwin, *Inorg. Chim. Acta*, 1977, **25**, L74.
13 B. N. Figgis, J. M. Patrick, P. A. Reynolds, B. W. Skelton, A. H. White and P. C. Healy, *Aust. J. Chem.*, 1983, **36**, 2043.
14 E. H. Witten, W. M. Reiff, K. Lazar, B. W. Sullivan and B. M. Foxman, *Inorg. Chem.*, 1985, **24**, 4585.
15 P. C. Healy, J. M. Patrick, B. W. Skelton and A. H. White, *Aust. J. Chem.*, 1983, **36**, 2031.
16 P. C. Healy, B. W. Skelton and A. H. White, *Aust. J. Chem.*, 1983, **36**, 2057.
17 M.-N. Collomb Dunand-Sauthier, A. Deronzier, C. Duboc-Toia, M. Fontecave, K. Gorgy, J.-C. Lepretre and S. Ménage, *J. Electroanal. Chem.*, in the press.
18 S. Ménage, J.-M. Vincent, C. Lambeaux, G. Chottard, A. Grand and M. Fontecave, *Inorg. Chem.*, 1993, **32**, 4766.
19 G. M. Sheldrick, SHELXTL version 5.1., Siemens Analytical X-Ray Instruments, Madison, WI, 1990.
20 C. Duboc-Toia, S. Ménage, J.-M. Vincent, M. T. Averbuch-Pouchot and M. Fontecave, *Inorg. Chem.*, 1997, **36**, 6148.
21 H. Sugimoto and D. T. Sawyer, *J. Org. Chem.*, 1985, **50**, 1784.
22 G. Cauquis, A. Deronzier, B. Sillon, B. Damin and J. Garapon, *J. Electroanal. Chem.*, 1981, **117**, 139.
23 S. Ménage, J.-M. Vincent, C. Lambeaux and M. Fontecave, *J. Mol. Catal. A Chem.*, 1996, **113**, 61.
24 P. A. Mac Faul, K. U. Ingold, D. D. Wayner and L. Que, Jr., *J. Am. Chem. Soc.*, 1997, **119**, 10594.
25 S. Ménage, E. C. Wilkinson, L. Que, Jr. and M. Fontecave, *Angew. Chem., Int. Ed. Engl.*, 1995, **34**, 203.

Paper 9/01893J